Equilibrium chemistry calculations for lean and rich hydrocarbon-air mixtures

S. M. Aithal
Mathematics and Computer Science Division, Argonne National Laboratory,
9700 S. Cass Ave., Argonne, IL 60439, USA

Phone # 630-252-3164, e-mail: aithal@mcs.anl.gov

Abstract: Chemical equilibrium calculations provide useful estimates of combustion products in a wide range of reacting flow systems. Such computations can be particularly useful in studying the performance, emissions, and NO_x abatement strategies in internal combustion engines with alternative fuels or in developing new engine operating regimes. Furthermore, such computations can provide useful information in comparing emissions of engines with different additives such as natural gas or methanol. This paper describes chemical equilibrium calculations conducted by using a set of reactions and species relevant to a wide range of combustible fuel-additive-air mixtures, using the equilibrium constant method. The chemical equilibrium system under consideration included 16 reactions and 20 species. The reaction set included reactions responsible for formation of NO_x along with reactions believed to be responsible for soot formation in rich fuel-air mixtures. The Newton-Raphson method was used for solving the nonlinear system of equations describing the formation of equilibrium products in reacting fuel-additive-air mixtures. The effect of temperature, pressure, and composition for various fuel-additive-air mixtures was studied. The Newton-Raphson scheme was found to be a robust and fast method for computing chemical equilibrium concentrations for a wide range of operating conditions such as temperature, pressure, and composition of fuel-additive-air mixtures. Equilibrium assumptions provided a good estimate of engine-out NOx and predicted other well-

known NOx formation trends in engines. Equilibrium assumptions also were shown to underpredict CO concentrations, especially with fuel-lean operating conditions

Keywords: equilibrium, dual-fuel, NO_x, emissions

Nomenclature

Greek Symbols

φ	equivalence ratio
θ	crank angle
υ	stoichiometric coefficient

Abbreviations

ATDC	after top dead center
BDC	bottom dead center
EGR	exhaust gas recirculation
EVO	exit valve open
SI	spark ignition
TDC	top dead center

1 Introduction

Combustion of hydrocarbons in power-generating equipments, such as gas turbines or internal combustion engines in automobiles, is a major source of air pollution. The combustion products formed from burning fuel-air mixtures contain oxides of nitrogen (NO, NO_2, and N_2O) along with CO, CO_2, and other organic compounds that are unburned or partially unburned hydrocarbons. The relative amounts of these pollutants, usually on the order of several hundred parts per million (PPM), depend on various factors including composition of the fuel-air mixture

and the operating conditions. Optimizing performance (power and efficiency), while minimizing emissions such as NO_x and soot, leads to conflicting design constraints. Development of fast and robust tools for computing the equilibrium concentration of products in the combustion chamber can play an important role in the design and optimization of combustors such as gas turbines and internal combustion engines. The need for such tools has been spurred by the renewed interest in flexible-fuel, or dual-fuel, engines. In these dual-fuel engines a combination of fuel-additive-air mixtures is used [1, 2]. The main fuel can be gasoline or diesel, and the additives can be natural gas (methane), hydrogen, acetylene, or alcohols (methanol or ethanol). A comparison of the emission characteristics of different fuel-additive combinations can help in the design and development of such flexible-fuel engines. A chemical equilibrium scheme that includes species and elementary reaction processes describing fuel combustion and formation of NO_x and soot would thus be an invaluable tool in the design and analyses of combusting systems.

Chemical equilibrium of a closed reacting system at a given pressure and temperature can be computed by minimizing the Gibbs free energy of the system or by using the approach of equilibrium constants using a set of reactions [3]. While these two formulations are equivalent and reduce to the same number of iteration equations [3 and references therein], each approach has its advantages and disadvantages. Minimization of the Gibbs free energy involves treating each species independently and does not require a set of reactions to be prescribed a priori. The details of the problem formulation and implementation using this approach are explained in [3]. For most combustion problems of interest to engineering applications, however, the equilibrium constant method is easier to formulate and implement. More important, the method can be easily coupled to quasi-dimensional codes to obtain equilibrium concentration of various species during the compression and expansion strokes.

Several authors have studied equilibrium chemistry calculations using a small set of species (typically 6–13) [4-8, and references therein]. Rashidi [4] studied a system with 13 species. Sample results were presented for hydrocarbons with an H/C ratio of 2, for a set of prescribed temperature and pressure. The numerical approach involved separating the species into two groups: species with relatively large concentrations (CO_2, H_2O, CO, H_2, O_2, and N_2) and species with lower concentrations (OH, NO, O, H, N_2O, NO_2, and N). Concentrations of those species with high values were determined first, by using the Newton-Raphson method. Following this step, the remaining species were determined with the successive substitution method. The two methods were iterated alternatively until the change in values was small. Details of the initial conditions or the total computational time were not explicitly described. This method is likely to be unsuitable for computing the temporal variation of species concentrations in engines, however, since the initial charge consists of a fuel-air mixture with little or no CO_2, H_2O, and H_2 (unless EGR is used). Furthermore, for stoichiometric and rich mixtures, O_2 concentrations tend to zero at equilibrium and hence cannot be included in the list of species with large concentrations. Given these limitations, the methodology presented in [4] would be of limited usefulness in studying temporal variation of equilibrium products during an actual engine cycle.

Rakopoulos et al. [5] used 11 species to describe the combustion products of diesel engines. The diesel fuel was modeled as n-dodecane. The 11x11 system of nonlinear equations was reduced to a 4x4 system by algebraic manipulation. The procedure of reducing the system of equations was ad hoc, however, and hence would be cumbersome if one were required to study a different fuel (other than n-dodecane) or a combination of fuels (as in dual-fuel engines). The resulting 4x4 system was solved by using the Newton-Raphson method to obtain equilibrium

concentration of the products. Results for a range of temperature, pressure, and equivalence ratios were presented for n-dodecane.

References [4] and [5] do not include reactions to model soot formation in rich mixtures (equivalence ratios > 3). Moreover, while the authors present sample results of the equilibrium products of hydrocarbon combustion, neither of the works discusses the application of the techniques to interpret actual engine data.

The goal of this work was to develop a fast, robust, and general-purpose tool and to use it to study the equilibrium reaction products for a wide-range of fuels-additive-air mixtures of relevance to a range of combustors. In order to accomplish this goal, a general set of reactions relevant to combustion systems, consisting of 20 species, was used (see Tables Table **1** Table 2). Reaction pathways based on phenomenological soot models as described in [9] were also included; these pathways are useful in studying combustors with spray injection (such as diesel engines). In the heterogeneous combustion phase during droplet break-up, it is believed that there are low-temperature pockets of fuel-air mixtures where the equivalence ratios are between 3 and 5. This is especially true in diesel engines operating under high-EGR conditions. The Newton-Raphson scheme was used to solve the 20x20 system of nonlinear equations. This scheme allows the tool to be used to study any fuel-additive combination where the fuel is of the form C_xH_y and the additive is of the form $C_{x1}H_{y1}O_{z1}$ without any modification of the set of equations. The tool was validated was and then used to study the impact of mixture composition, temperature, and pressure on equilibrium concentration of combustion products. Furthermore, the tool was applied to examine the emission characteristics of a natural gas and dual-fuel diesel engines.

This paper is organized as follows. Section 2 discusses the mathematical formulation used in this work. Section 3 discusses validation of the Newton-Raphson solver used to compute the

equilibrium concentrations. Also discussed are the computational time required for typical equilibrium computations and the application of the equilibrium chemistry computations for various case studies. Section 4 presents important conclusions and observations about this work.

2 Mathematical formulation

Given a chemical reaction of the form

$$\upsilon_a A + \upsilon_b B \leftrightarrow \upsilon_c C + \upsilon_d D \tag{1}$$

the equilibrium constant k_p can be written as

$$k_p = \frac{\left(P_c\right)^{\upsilon_c}\left(P_d\right)^{\upsilon_d}}{\left(P_a\right)^{\upsilon_a}\left(P_b\right)^{\upsilon_b}} \tag{2}$$

Since the partial pressure of species A is related to the mole fraction (x_a) as

$$P_a = x_a P \tag{3}$$

one can write the constant as

$$k_p = \frac{\left(x_c\right)^{\upsilon_c}\left(x_d\right)^{\upsilon_d}}{\left(x_a\right)^{\upsilon_a}\left(x_b\right)^{\upsilon_b}} P^{\upsilon_c+\upsilon_d-\upsilon_a-\upsilon_d=} \tag{4}$$

Following the treatment in standard thermodynamic textbooks,

$$\ln k_p = \frac{-1}{RT}\sum_{1}^{s} \upsilon_i \left(\Delta G_f^{\circ}(T)\right)_i \tag{5}$$

where $\Delta G(T)_i$ was computed by using the procedure outline in [10]. The thermodynamic coefficients required for the temperature-dependent entropy and the enthalpy of individual species were computed by using CHEMKIN coefficients. For each reaction given in Table 2, the reaction rate was calculated at the prescribed temperature and pressure (P) as shown in Eq. (5). Table 2 also shows the nonlinear equations describing the relationship between the mole-fraction and equilibrium rate constants as described in Eq. (2). These 16 nonlinear equations, along with the atom conservation equation for C, H, O, and N, were used to obtain the concentration of each of the 20 species considered in this work. The system of 20x20 equations was solved y using the Newton-Raphson method.

3 Method

The main emphasis of this work was to develop a fast and robust method to compute equilibrium concentration of products formed as a result of combustion of various fuel-additive-air mixtures. The operating conditions and compositions were chosen to assess the ability of the model to predict NO_x formation in engines operating with different fuel-additive-air mixtures. As shown in Table 1, C_xH_y, represents the fuel (such as diesel, which is modeled as n-heptane), and $C_{x1}H_{y1}O_{z1}$ represents an additive (such as CH_4 or CH_3OH). The numerical framework used in this work was set up such that the user specifies the values of x, y, x_1, y_1, and z_1, so as to identify the fuel and additive. The constants required for the computations of the thermophysical properties (such as enthalpy and internal energy) for each species were read in from the database and used to compute the Gibbs free energy and equilibrium constants for the reactions shown in Table 2. This setup allows the user to test various fuel-additive combinations without any code modifications and hence enhances its utility as a design tool.

4 Results and Discussion

This section focuses on three aspects: validation and verification of the Newton-Raphson solver, the computational time required for the simulations, and four case studies in which the equilibrium concentrations of combustion products for various fuel-additive-air mixtures were obtained.

4.1 Validation and verification of the Newton-Raphson solver

Table 3 through Table 5 show the initial conditions—temperature, pressure and species concentration—for the pentane-methanol-air mixtures, pentane-methane-air mixtures, and rich

pentane-air mixtures. All computations were conducted by using the constant pressure, constant temperature constraint. The results computed by using the Newton-Raphson solver in this work are in excellent agreement with those computed by using STANJAN [11], thus validating the Newton-Raphson solver.

4.2 Computation time required for the simulation

Robustness and computational time are important considerations for design and analysis tools. The Newton-Raphson method was found to be robust and computationally fast for the system of 20x20 coupled equations considered in this work.

For lean fuel-additive-air mixtures, obtaining equilibrium concentrations at a prescribed temperature and pressure typically took about 10–20 iterations, requiring a total time of less than 1 millisecond on single-CPU 3 GHz machine. An entire sequence of calculations for the compression/expansion stroke of a typical engine cycle took about 100 milliseconds. The computations are much faster than computations conducted with CHEMKIN/STANJAN, which take on the order of 3–15 seconds for each equilibrium calculation.

Equilibrium calculations of rich mixtures take about 50–250 iterations, depending on temperature, pressure and operating conditions. The time required for computing the equilibrium concentration of a rich fuel-air mixture for a single prescribed value of temperature and pressure was on the order of 10–20 milliseconds.

The ability of the present numerical framework to rapidly compute equilibrium concentrations of a wide range of fuel-additive air mixtures at various temperature, pressure, and species compositions makes it a valuable design and optimization tool.

4.3 Case studies

The equilibrium chemistry calculations were used to compute equilibrium products for a wide variety of fuel-additive-air mixtures at different temperatures and pressures, representing different engines and engine operating conditions. Equilibrium concentrations of combustion products such as NO_x and CO were compared with experimental data in order to assess the accuracy of equilibrium assumptions in predicting the formation of pollutants under actual engine operating conditions.

4.3.1 Full-cycle NOx and CO calculations in natural gas engines: Stationary large-bore engines fueled by natural gas are used in applications such as power generation and gas transmission. Since such engines are used for long durations, optimizing their performance and emissions is essential. NO_x and CO emissions from such engines can be analyzed by using the strategy outlined below and can be useful in assessing various NO_x abatement strategies. Knowing the temporal variation of pressure, engine geometry, and flow rates of the fuel and air, one can compute the temporal variation of average temperature in the engine cylinder. The average cylinder temperature at a given crank angle θ is given by $T(\theta) = \frac{P(\theta)V(\theta)}{mR_g(\theta)}$, where $R_g(\theta)$ is the gas constant and m is the total mass of the working fluid (unburned fuel, air, and combustion products) at a given crank angle. Knowing the composition of the fuel-air mixture at the start of the compression stroke, along with the temporal variation of pressure and temperature, one can obtain the equilibrium composition of the combustion products at each crank angle. The species concentration at each crank-angle serves as the initial concentration for the calculation of equilibrium products at the pressure and temperature at the next crank angle. Figure 1(a) shows

experimental pressure profiles for the 0% NEA spark-ignition case discussed in [12] for two equivalence ratios, $\varphi = 1.0$ and $\varphi = 0.65$. Figure 1(b) shows the temporal variation of average cylinder temperature calculated by using the procedure discussed above. The case with $\varphi = 0.65$ has a higher fuel-air mass and hence a lower overall average temperature than that of the $\varphi = 1.0$ case, despite the higher cylinder pressure shown in Figure 1(a). Methane (CH_4) was used to represent natural gas in the equilibrium chemistry computations. As seen in Figure 1(c), the equilibrium NO_x production follows the temperature variation, with NO_x values for the $\varphi = 1$ case being higher than the $\varphi = 0.65$ case. As the temperature and pressure of the working fluid decrease during the expansion stroke, the NO_x concentration drops sharply. The NO_x concentration is believed to freeze a few crank-angle degrees after combustion is complete (typically around 35°–50° ATDC). For lean mixtures, the combustion duration is longer than for near-stoichiometric mixtures. The NO_x concentration shown in Figure 1(c) around 35° ATDC is about 3000 PPM for $\varphi = 1$ and about 2000 PPM for $\varphi = 0.65$ at 50° ATDC. These values are typical of natural gas engines operating under conditions reported in [12]. Figure 1(d) shows the temporal variation of CO throughout the engine cycle for several values of equivalence ratios. At the end of combustion ($\theta > 35$ ATDC), there is a steep drop in the CO concentration as the equivalence ratio changes from stoichiometric to fuel-lean ($\varphi = 0.9$), followed by a less pronounced drop in CO concentration for smaller values of the equivalence ratio φ. These characteristics are similar to the engine-out CO measurements reported in [12]. However, the overall drop in CO from $\varphi = 1$ to $\varphi = 0.65$ is about a factor of 30, whereas equilibrium computations show a much larger drop in CO concentration at a given crank angle, as shown in Figure 1(d). For instance, at a crank angle of 40°, the concentration of CO is about 6000 PPM for $\varphi = 1$, whereas it is about 20 PPM at $\varphi = 0.65$. This could be due to the following reasons: either

CO formation is more strongly influenced by finite-rate kinetics, or CO formation freezes earlier in the expansion stroke as the equivalence ratio decreases from $\varphi = 1.0$ to $\varphi = 0.65$. Equilibrium concentrations of C, C_2H_2, CH_3, and HCN were also negligible (< 1.0E-5 PPM) for temperatures and pressures typical of near-TDC conditions (T = 2500 K and P = 50 atm) and also at conditions typical of EVO conditions (T = 1000K and P = 5 atm). These observations suggest that equilibrium assumptions may be unsuitable for predicting engine-out concentrations of CO, soot, and soot-forming precursors (C, C_2H_2, CH_3) in lean mixtures.

4.3.2 Equilibrium concentration of fuel-rich hydrocarbon mixtures: Modern diesel engines use exhaust-gas recirculation for NO_x control. Introduction of EGR leads to reduced combustion flame temperature and hence a reduction of NO_x. However, the combined effect of reducing charge-gas oxygen and combustion temperatures leads to incomplete combustion and increased particulate matter emissions. Since diesel fuel can be closely approximated by n-heptane, it is instructive to study the effect of equivalence ratio on species concentrations. Figure 2 shows important species concentrations in rich pentane and n-heptane mixtures at T = 2200 K and P = 80 atm. The equilibrium concentrations of various species for both pentane and n-heptane exhibit similar characteristics. As expected, there is a marked increase in CO and H_2 (almost 2 orders of magnitude) as the equivalence ratio φ increases above 1 (fuel rich). HCN and C_2H_2 become important beyond an equivalence ratio of 3.5. Figure 3 shows the effect of temperature and pressure on the formation of C_2H_2 and HCN in fuel-rich n-heptane air mixtures. During the rich premixed burn phase the equivalence ratio is believed to be between 2 and 5 [13] and hence chosen for this study. The set of conditions corresponding to T = 1500 K, P = 35 atm represents conditions after the beginning of the fuel injection in a typical diesel engine, whereas T = 2200, P = 80 atm corresponds to conditions near TDC toward the end of the fuel injection process. At

equivalence ratios below $\phi = 3$, formation of HCN and C_2H_2 is negligible. However, the concentration of these species increases dramatically beyond $\phi = 3$. As expected, at lower temperatures and pressures, the equilibrium concentration of C_2H_2, the precursor for soot formation, is higher, but it drops as the temperature and pressure increase during the compression stroke. At higher temperatures and pressures, the concentration of HCN increases as compared to its value at a lower temperature. Using such equilibrium calculations at various operating conditions of temperature and pressure, designers can evaluate the impact of high EGR on the formation of soot.

4.3.3 NO_x formation in fuel-lean diesel engines: The impact of fuel-lean operation and EGR fraction is an important consideration in the design of diesel engines from the standpoint of optimizing performance and reducing emissions. Equilibrium chemistry calculations were conducted for a range of equivalence ratios and EGR fractions for n-heptane (representative of diesel fuel). The initial molar concentration of fuel (C_7H_{16}), O_2, N_2, CO_2, and H_2O for various equivalence ratios and % EGR fractions were computed by using Eq. 6 in [14]. As an example, **Error! Reference source not found.** shows the initial concentration of fuel-air for a stoichiometric mixture with no EGR and a fuel-air-EGR mixture with 20% EGR and an equivalence ratio of 0.8. NO_x formation for a particular fuel-air-EGR mixture was computed at the mixture explosion temperature as explained in [15]. The initial enthalpy of the mixture was computed at 700 K. This is the typical mixture temperature when fuel injection begins in diesel engines and hence was chosen as the temperature to compute the initial enthalpy of the fuel-air-EGR mixture. The temperature at which the enthalpy of the equilibrium composition matched the initial mixture enthalpy was defined as the mixture explosion temperature. As is well known, the initial NO_x formation is primarily proportional to the stoichiometric adiabatic flame

temperature [16]. Increasing the EGR fraction or oxygen concentration (lower values of equivalence ratio) lowers the stoichiometric adiabatic flame temperature and hence the mixture explosion temperature. The mixture explosion temperature is thus an appropriate temperature value to compare equilibrium NO_x concentrations, since this is the maximum temperature attained by a given fuel-air-EGR mixture. Figure 4 shows the NO_x formation at the mixture explosion temperature for various values of %EGR and equivalence ratios. Figure 5 shows the effect of ϕ on the mixture explosion temperature for various % EGR values. As expected, Figure 4 shows that the peak NO_x formation for all EGR fractions occurs close to an equivalence ratio of 0.8. This behavior is well known in engines and is due to two opposing effects: a drop in mixture explosion temperature (as shown in Figure 5) and an increase in the O_2 concentration as the mixture is leaned out, giving a peak NO_x concentration at $\phi \approx 0.8$. This behavior can be explained by observing the mixture explosion temperatures shown in Figure 5. Figure 5 shows that for a given value of ϕ, a higher value of % EGR leads to a lower mixture explosion temperature and hence a lower value of NO_x as seen in Figure 4. Figure 5 also shows that as the equivalence ratio drops, so does the mixture explosion temperature. The relative effects of % EGR and equivalence ratios on equilibrium NO_x can be correlated to engine-out NO_x and can aid in the design and optimization of the range of operating conditions.

4.3.4 Dual-fuel diesel engines: Dual-fuel engines operate on both natural gas and diesel fuel simultaneously. The majority of the fuel burned is natural gas, whereas diesel fuel is used to ignite the mixture. This strategy allows retention of the diesel compression ratio and the associated higher efficiency while burning cheap and clean natural gas. Dual-fuel engines can run on either liquid natural gas or compressed natural gas. Both fuels have relatively high octane numbers, which lead to performance improvements. Furthermore, engines running natural gas

with diesel typically have 20% to 30% less CO_2 emissions. Dual-fuel engines can also be run on a variety of other gaseous fuels such as C_2H_2, H_2, and CH_3OH. Experimental studies of such engines have been reported by various groups [17-19]. Dual-fuel engines can also be operated in the straight diesel mode, if need be, which greatly enhances its utility as a flexible fuel engine. Given these desirable features of dual-fuel engines, their design and optimization would benefit greatly if designers could evaluate the relative effects of the fuel-type, engine load, and speed on emissions. For instance, Lakshmanan and Nagarajan [18] report a 24% increase in NO_x emissions with a C_2H_2/diesel operation, while Papagiannakis et al. [17] report a reduction in NO_x with a CH_4/diesel operation. By studying the effect of temperature on the diesel-additive combination, some estimates of the impact of fuel-additive ratio on NO_x emissions can be obtained. Figure 6 shows the effect of temperature on the equilibrium NO_x concentration for various combinations of n-heptane and natural gas (CH_4). The number of moles of n-heptane and CH_4 is varied so as to maintain a constant value of enthalpy corresponding to a case of neat stoichiometric diesel operation (1 mole of n-heptane, 0 moles of CH_4). It is seen that a stoichometric n-heptane/CH_4 mixture with 0.1 moles of n-heptane and 1.457 moles of CH_4 has about a 5% lower NO_x concentration at conditions close to TDC (2000–2200 K) as compared to the case with neat diesel. As expected, an intermediate case with 0.5 moles of n-heptane and 0.78 moles of CH_4 results in less reduction of NO_x concentration.

In addition to such theoretical computations, the equilibrium chemistry solver can be used to analyze and estimate NO_x emissions for actual engine operating conditions. Sample calculations were conducted to assess NO_x concentrations predicted by equilibrium computations with experimental data reported in [17]. Using the geometrical details of the single-cylinder, naturally aspirated engine, the initial cylinder composition was computed assuming a cylinder

pressure of 0.85 atm at BDC for various values of diesel fuel supplementary ratio (x) and total relative air-fuel ratio (λ) as defined in [17]. Figure 7 shows a comparison of NO_x concentration predicted by the equilibrium solver with experimental data reported in [17] corresponding to an engine speed of 1500 RPM, for three loads (BMEP). Since details about the temporal variation of pressure are not described in [17], equilibrium computations were conducted at a pressure of 20 atm. It was verified that the NO_x concentrations were a weak function of pressure at a given temperature (about 1.5% difference over a pressure difference of 10 atm). At each value of x and λ (corresponding to a given load), equilibrium computations were performed for a range of temperatures from 1000 K to 2000 K. It was seen that the NO_x concentrations at temperatures of 1250 K, 1350 K, and 1450 K for engine loads (BMEP) of 1.2, 2.4, and 3.7 bar, respectively, matched values reported in [17]. These temperature values are representative of average gas temperature in the diesel engine a few crank-angle degrees after fuel combustion is complete. The increasing value of NO_x formation temperature with load is also consistent with the increasing values of exhaust temperature reported in [17].

Figure 8 shows CO concentration over a range of temperatures for three values of load and mixture composition (x and λ). The CO concentration predicted equilibrium assumptions is less than 1 g/kWh even for temperatures as high as 2000 K, whereas the CO concentrations reported in [17] lie between 1 and 100 g/kWh. This result is consistent with the earlier observation that equilibrium assumptions greatly underpredict CO concentrations, especially for fuel-lean conditions. Concentrations of C, C_2H_2, HCH, and C_7H_{15} were also negligible (similar to equilibrium compositions noted with the natural gas engine computations).

5 Conclusions

Chemical equilibrium calculations were conducted with a set of reactions and species relevant to a wide-range of combustible fuel-additive-air mixtures. The effect of temperature, pressure, and composition for various fuel-additive-air mixtures was studied by using the equilibrium constant method. The Newton-Raphson method was found to be a fast and robust technique for solving the system of nonlinear equations describing the formation of equilibrium products in reacting fuel-additive-air mixtures. The equilibrium chemistry computations yielded results that agree well with NO_x formation trends observed in diesel and SI engines. It was also seen that equilibrium assumptions underpredicted CO concentrations especially in engines with lean-fuel mixtures. Similarly, equilibrium concentrations of species believed to be precursors in soot formation such as C, C_2H_2, and HCN were found to be negligible in fuel-lean conditions. These observations suggest that equilibrium computations have the potential to provide good estimates of engine-out NO_x in a wide variety of engines and to assist in the evaluation of various NO_x abatement strategies. The results of this work also suggest that prediction of CO and soot in fuel-lean conditions might require more detailed finite-rate chemical kinetic computations.

Acknowledgments: The author thanks Dr. S. Som for helpful discussion during this work. The submitted manuscript has been created by UChicago Argonne, LLC, Operator of Argonne National Laboratory ("Argonne"). Argonne, a U.S. Department of Energy Office of Science laboratory, is operated under Contract No. DE-AC02-06CH11357.

References

1. Wallner, T., Miers, S. A., McConnell, S., "A comparison of ethanol and butanol as oxygenates using a direct-injection, spark-ignition engine," J. Eng. Gas Turbines Power 131(3) (2009).
2. Wallner, T., Frazee, R., "Study of regulated and non-regulated emissions from combustion of gasoline, alcohol fuels and their blends in a DI-SI engine," SAE paper 2010-01-1571, 2010.
3. Gordon, S. and McBride, B. I., "Computer program for calculation of complex chemical equilibrium compositions and applications," NASA Reference Publication 1311, Oct. 1994.
4. Rashidi, M, "Calculation of equilibrium composition in combustion products," Chem. Eng. Technol. 20 (1997) 571–575.
5. Rakopoulos, C. D., Hountalas, D. T., Tzanos E. I., G. N. Taklis, "A fast algorithm for calculating the composition of diesel combustion products using 11 species chemical equilibrium scheme," Advances in Engineering Software 19 (1994) 109-119.
6. Vickland, C. W., Strange, F. M., Bell, R. A., Starkman, E. S., "A consideration of the high temperature thermodynamics of internal combustion engines," Trans. SAE 70 (1962) 785 – 793.
7. Way, R. J. B., "Methods for determination of composition and thermodynamic properties of combustion products for internal combustion engines calculations," Inst. Mech. Engrs. 190 (1977) 687–697.
8. Olikara, C., Bofman, G. L., "A computer program for calculating properties of equilibrium combustion products with some applications to I.C. engines," SAE Paper 750468, 1975.

9. Tao, F. Srinivas, S., Reitz, R. D., Foster, D. E., "Comparison of three soot models applied to multi-dimensional diesel combustion simulations," JSME International Journal Series B 48(4) (2005) 671–678.
10. Kee, R. J. , Rupley, F. M, Meeks E, Miller, J. A., "CHEMKIN-III: A FORTRAN chemical kinetics package for the analysis of gas-phase chemical and plasma kinetics," Sandia technical report SAND96-8216, 1996.
11. http://navier.engr.colostate.edu/tools/equil.html
12. Biruduganti, M., Gupta, S., Bihari, B., McConnell, S., Sekar, R., "Air separation membranes – an alternative to EGR in large bore natural gas engines," ASME Internal Combustion Engine 2009 spring technical conference paper ICES2009-76054, 2009.
13. Dec, J. E., "A conceptual model of diesel combustion based on laser-sheet imaging," SAE paper 970873, 1997.
14. Aithal, S. M., "Impact of EGR fraction on diesel engine performance considering heat loss and temperature-dependent properties of the working fluid," Int. J. Energy Research 33(4) (2009) 415–430.
15. Strehlow, R. A., *Combustion Fundamentals*, McGraw-Hill, New York, 1984.
16. Heywood, J. B., *Internal Combustion Engine Fundamentals,* McGraw-Hill, New York, 1988.
17. Papagiannakis, R. G., Rakopoulos, C. D., Hountalas, D. T., Rakapoulos, D. C., "Emission characteristics of high speed, dual fuel, compression ignition engine operating in a wide range of natural gas/diesel fuel proportions," Fuel 89(7) (2010) 1397–1406.
18. Lakshmanan, T., Nagarajan, G., "Experimental investigation on dual fuel operation of acetylene in a DI diesel engine," Fuel Processing Technology 91(5) (2010) 496–503.

19. Lata, D. B., Misra, A., “Theoretical and experimental investigations on the performance of dual fuel diesel engine with hydrogen and LPG as secondary fuels,” Int. J. Hydrogen Energy 35(21) (2010) 11918 –11931.

Table 1: List of species

	Species*
1	C_xH_y (fuel)
2	$C_{x1}H_{y1}O$ (additive)
3	O_2
4	CO_2
5	H_2O
6	N_2
7	N
8	O
9	NO
10	OH
11	H
12	N_2O
13	CO
14	H_2
15	NO_2
16	HO_2
17	C
18	HCN
19	C2H2
20	C_xH_{y-1}

*x and y are the number of carbon and hydrogen atoms in the hydrocarbon; x_1, y_1, and z_1 are the hydrocarbon atoms in the additive.

Table 2: Elementary processes considered in this model

1	$\frac{1}{2}H_2 = H$	$k_1 = \frac{[H]}{[H_2]^{0.5}}\sqrt{P}$
2	$\frac{1}{2}O_2 = O$	$k_2 = \frac{[O]}{[O_2]^{0.5}}\sqrt{P}$
3	$\frac{1}{2}N_2 = N$	$k_3 = \frac{[N]}{[N_2]^{0.5}}\sqrt{P}$
4	$\frac{1}{2}H_2 + \frac{1}{2}O_2 = OH$	$k_4 = \frac{[OH]}{[H_2]^{0.5}[O]^{0.5}}$
5	$\frac{1}{2}N_2 + \frac{1}{2}O_2 = NO$	$k_5 = \frac{[NO]}{[N_2]^{0.5}[O]^{0.5}}$
6	$H_2 + \frac{1}{2}O_2 = H_2O$	$k_6 = \frac{[H_2O]}{[H_2][O]^{0.5}}$
7	$CO + \frac{1}{2}O_2 = CO_2$	$k_7 = \frac{[CO_2]}{[CO][O_2]^{0.5}}(P)^{-0.5}$
8	$NO + \frac{1}{2}O_2 = NO_2$	$k_8 = \frac{[NO_2]}{[NO][O_2]^{0.5}}(P)^{-0.5}$
9	$O_2 + \frac{1}{2}H_2 = HO_2$	$k_9 = \frac{[HO_2]}{[O_2][H_2]^{0.5}}(P)^{-0.5}$
10	$N_2 + \frac{1}{2}O_2 = N_2O$	$k_{10} = \frac{[N_2O]}{[N_2][O_2]^{0.5}}(P)^{-0.5}$
11	$C_xH_y + \left(x + \frac{y}{4}\right)O_2 = xCO_2 + \frac{y}{2}H_2O$	$k_{11} = \frac{[CO_2]^x[H_2O]^{0.5y}}{[C_xH_y][O_2]^{x+0.25y}}(P)^{(0.5y-1)}$
12	$C_{x1}H_{y1}O_{z1} + \left(x1 + \frac{y1}{4} - \frac{z1}{2}\right)O_2 = x1CO_2 + \frac{y1}{2}H_2O$	$k_{12} = \frac{[CO_2]^{x1}[H_2O]^{0.5y1}}{[C_{x1}H_{y1}O_{z1}][O_2]^{x1+0.25y1-0.5z1}}(P)^{(0.5y1-1-0.5z1)}$

13	$C_xH_y = C_xH_{y-1} + H$	$k_{13} = \frac{[C_xH_{y-1}][H]}{[C_xH_y]}P$
14	$2C_xH_{y-1} = xC_2H_2 + (y-x-1)H_2$	$k_{14} = \frac{[C_2H_2]^x[H_2]^{(y-x-1)}}{[C_xH_{y-1}]^2}(P)^{(y-3)}$
15	$C_2H_2 = 2C + H_2$	$k_{15} = \frac{[C]^2[H_2]}{[C_2H_2]}P^2$
16	$C_2H_2 + N_2 = 2HCN$	$k_{16} = \frac{[HCN]^2}{[C_2H_2][N_2]}$

Table 3: Validation of pentane-methanol mixtures

Temperature (K)	3200
Pressure (atm)	35
C_5H_{12} (moles)	1
CH_3OH (moles)	0.1
O_2 (moles)	8.15
N_2 (moles)	30.644
All other species	1.0E-30

	Species	Code (Mole Fraction)	STANJAN (Mole Fraction)
1	C_5H_{12}	1.186889E-58	0.0000E+00
2	CH_3OH	3.108337E-12	6.4634E-14
3	O_2	1.790785E-02	1.7911E-02
4	CO_2	6.401841E-02	6.4002E-02
5	H_2O	1.165357E-01	1.1653E-01
6	N_2	6.902252E-01	6.9022E-01
7	N	6.506663E-06	6.5026E-06
8	O	4.830986E-03	4.8321E-03
9	NO	1.701193E-02	1.7019E-02
10	OH	1.936549E-02	1.9366E-02
11	H	5.280299E-03	5.2794E-03
12	N_2O	4.841432E-06	4.8389E-06
13	CO	5.227207E-02	5.2288E-02
14	H_2	1.250074E-02	1.2501E-02
15	NO_2	1.308406E-05	1.3075E-05
16	HO_2	2.694174E-05	2.6933E-05

Table 4: Validation of pentane-methane-air mixtures

Temperature (K)	2500
Pressure (atm)	35
C_5H_{12} (moles)	1
CH_4 (moles)	1
O_2 (moles)	10
N_2 (moles)	37.6
All other species	1.0E-30

	Species	Code (Mole Fraction)	STANJAN (Mole Fraction)
1	C_5H_{12}	4.725217E-67	0.0
2	CH_4	3.531725E-15	3.5264E-15
3	O_2	3.992629E-03	3.9936E-03
4	CO_2	1.052205E-01	1.0522E-01
5	H_2O	1.500578E-01	1.5006E-01
6	N_2	7.218287E-01	7.2183E-01
7	N	4.168169E-08	4.1642E-08
8	O	1.533250E-04	1.5334E-04
9	NO	3.184135E-03	3.1852E-03
10	OH	2.748469E-03	2.7484E-03
11	H	2.063659E-04	2.0628E-04
12	N_2O	9.032364E-07	9.0274E-07
13	CO	1.021927E-02	1.0223E-02
14	H_2	2.383271E-03	2.3828E-03
15	NO_2	2.105280E-06	2.1039E-06
16	HO_2	2.439475E-06	2.4386E-06

Table 5: Validation of rich pentane-air mixtures (equivalence ratio = 5)

Temperature (K)	2200
Pressure (atm)	80
C_5H_{12} (moles)	5
CH_4 (moles)	0
O_2 (moles)	8
N_2 (moles)	30.08
All other species	1.0E-30

	Species	Code (Mole Fraction)	STANJAN (Mole Fraction)
1	C_5H_{12}	4.725217E-67	
2	CH_4	3.531725E-15	3.5264E-15
3	O_2	3.992629E-03	3.9936E-03
4	CO_2	1.052205E-01	1.0522E-01
5	H_2O	1.500578E-01	1.5006E-01
6	N_2	7.218287E-01	7.2183E-01
7	N	4.168169E-08	4.1642E-08
8	O	1.533250E-04	1.5334E-04
9	NO	3.184135E-03	3.1852E-03
10	OH	2.748469E-03	2.7484E-03
11	H	2.063659E-04	2.0628E-04
12	N_2O	9.032364E-07	9.0274E-07
13	CO	1.021927E-02	1.0223E-02
14	H_2	2.383271E-03	2.3828E-03
15	NO_2	2.105280E-06	2.1039E-06
16	HO_2	2.439475E-06	2.4386E-06

Table 6: Initial concentration of mixtures for computing equilibrium concentrations

	Species	Moles $\phi = 1$, EGR = 0%	Moles $\phi = 0.8$, EGR = 20%
1	C_7H_{16}	1	1
2	O_2	11	14.3
3	CO_2	0	1.4
4	H_2O	0	1.6
5	N_2	41.355	62.085

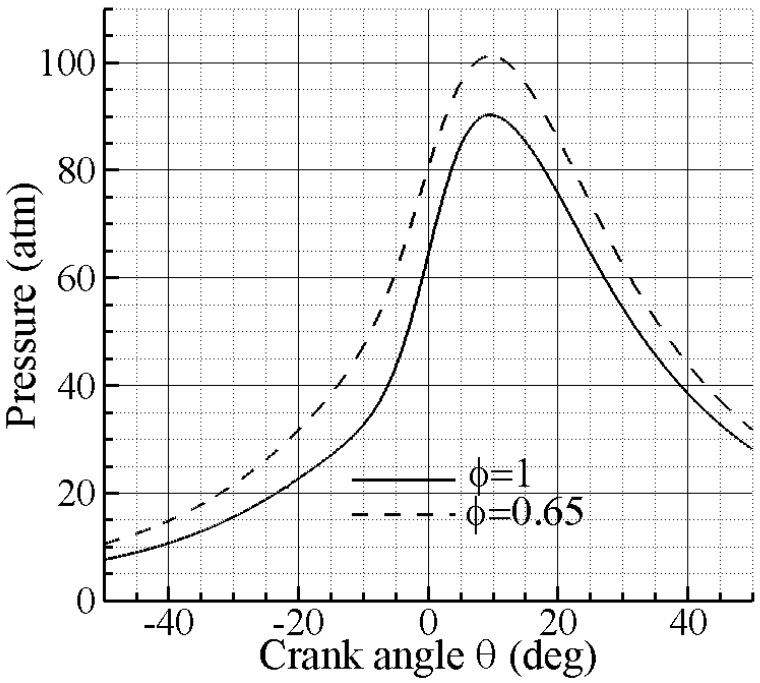

(a)

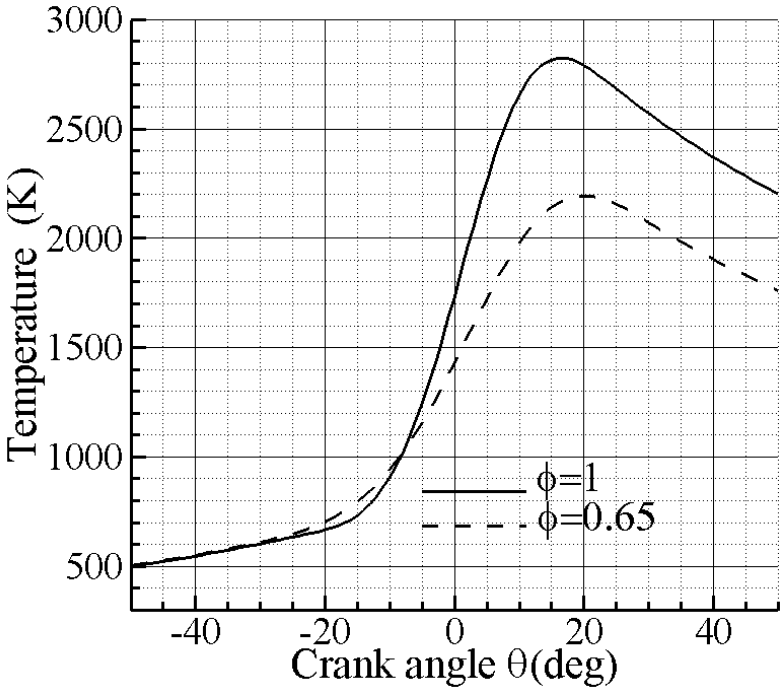

(b)

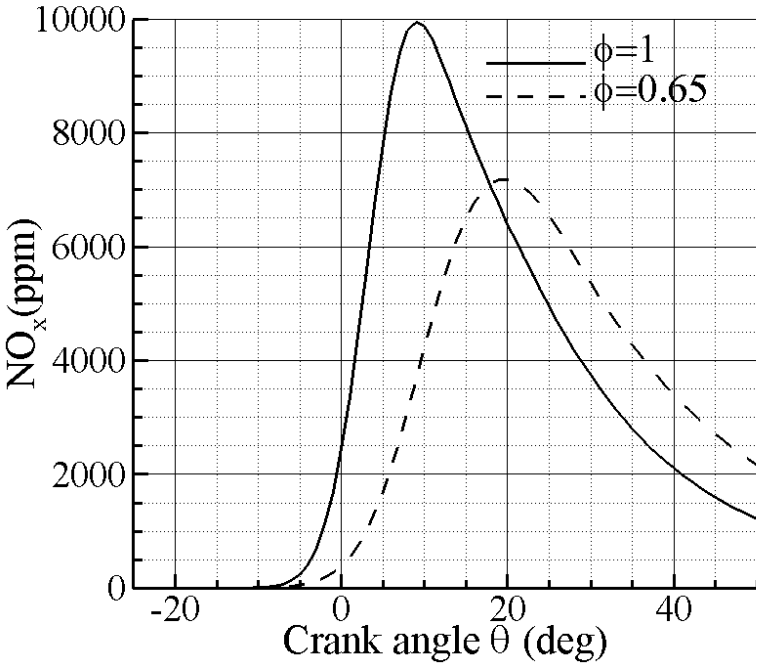

(c)

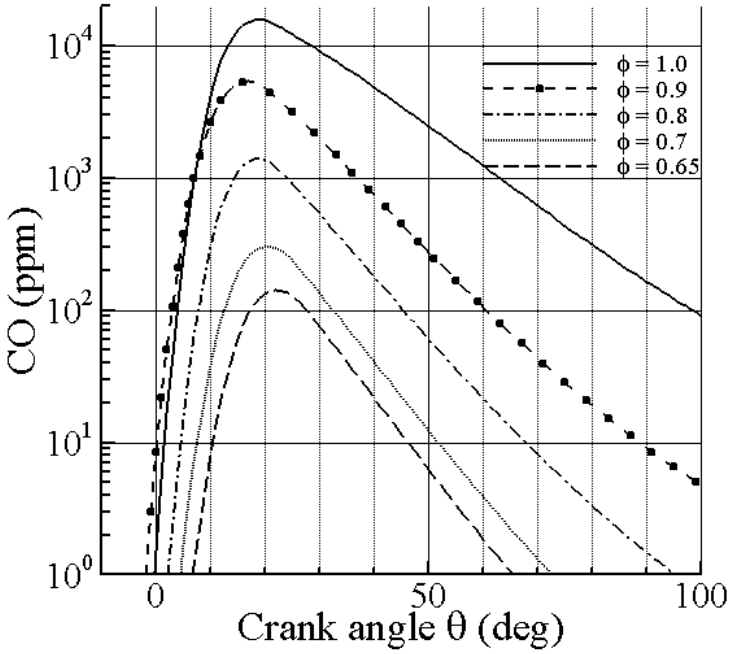

(d)

Figure 1: Temporal variation of pressure, temperature, NO_x, and CO in a natural gas engine.

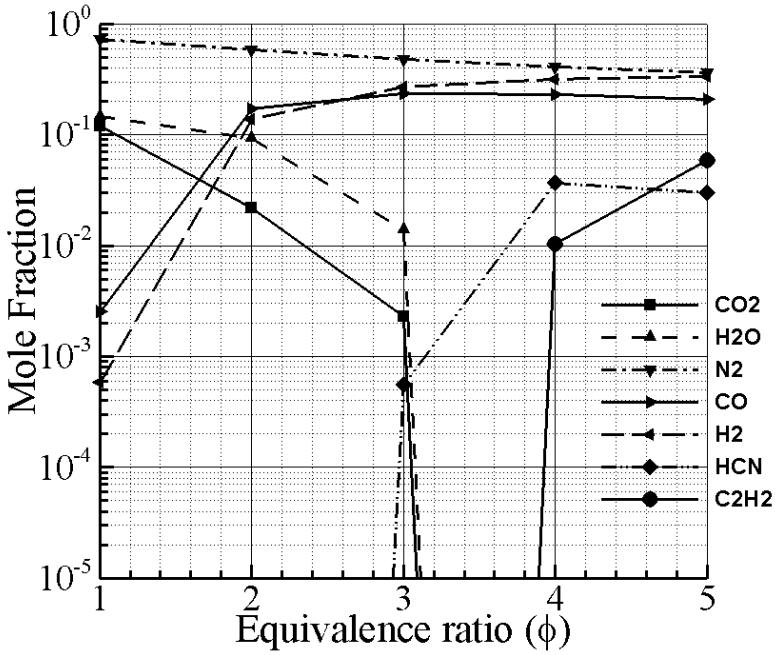

(a)

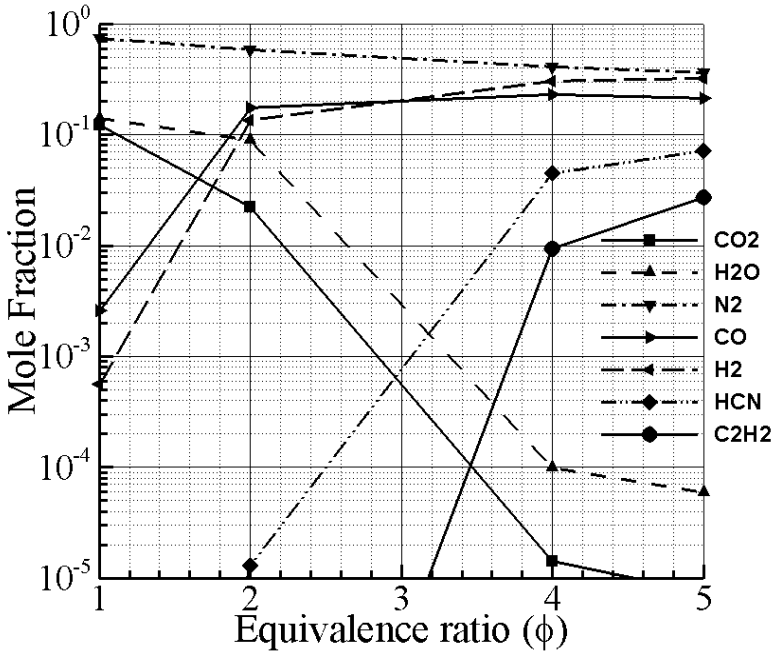

(b)

Figure 2: Effect of equivalence ratio (ϕ) on species concentration: (a) pentane, (b) n-heptane.

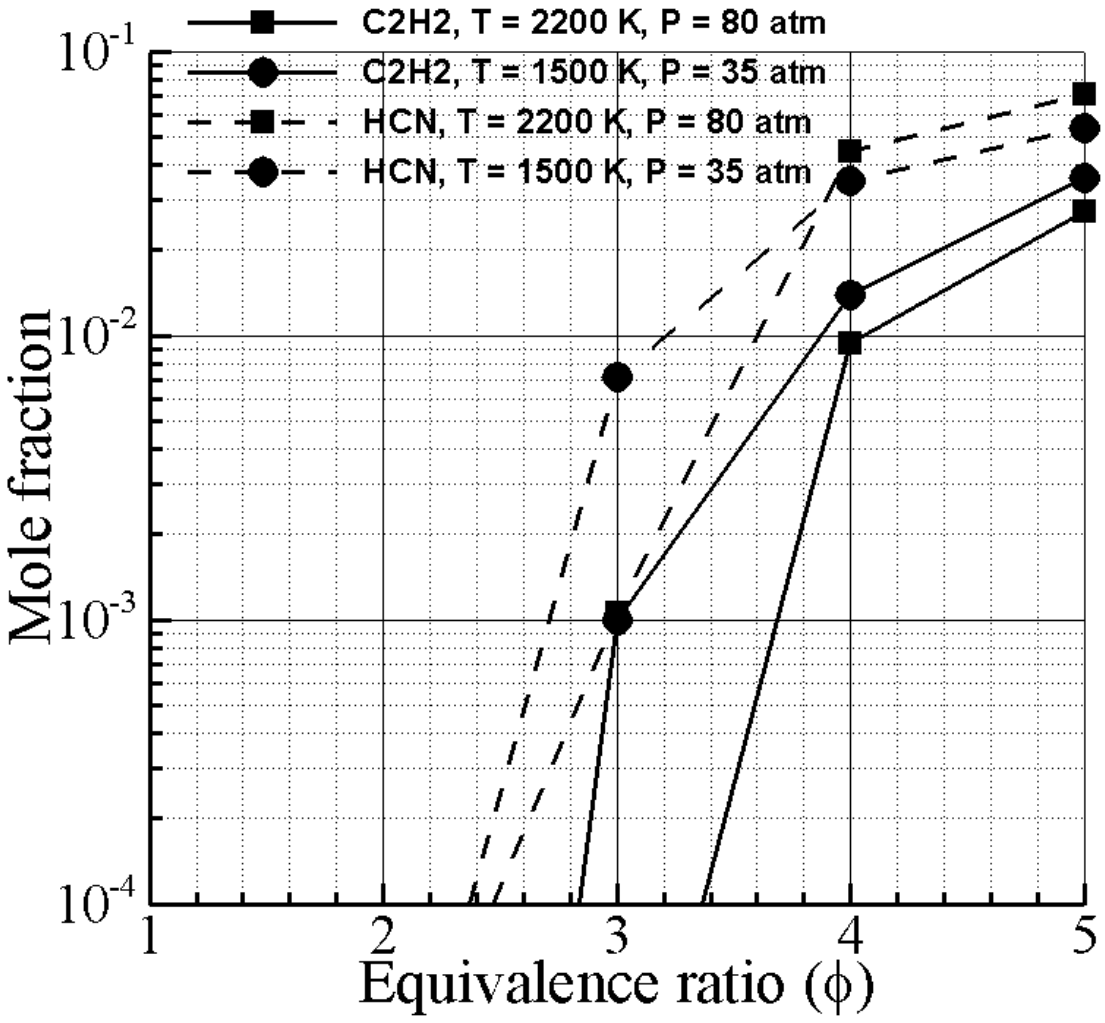

Figure 3: Effect of temperature and pressure on the formation of HCN and C_2H_2.

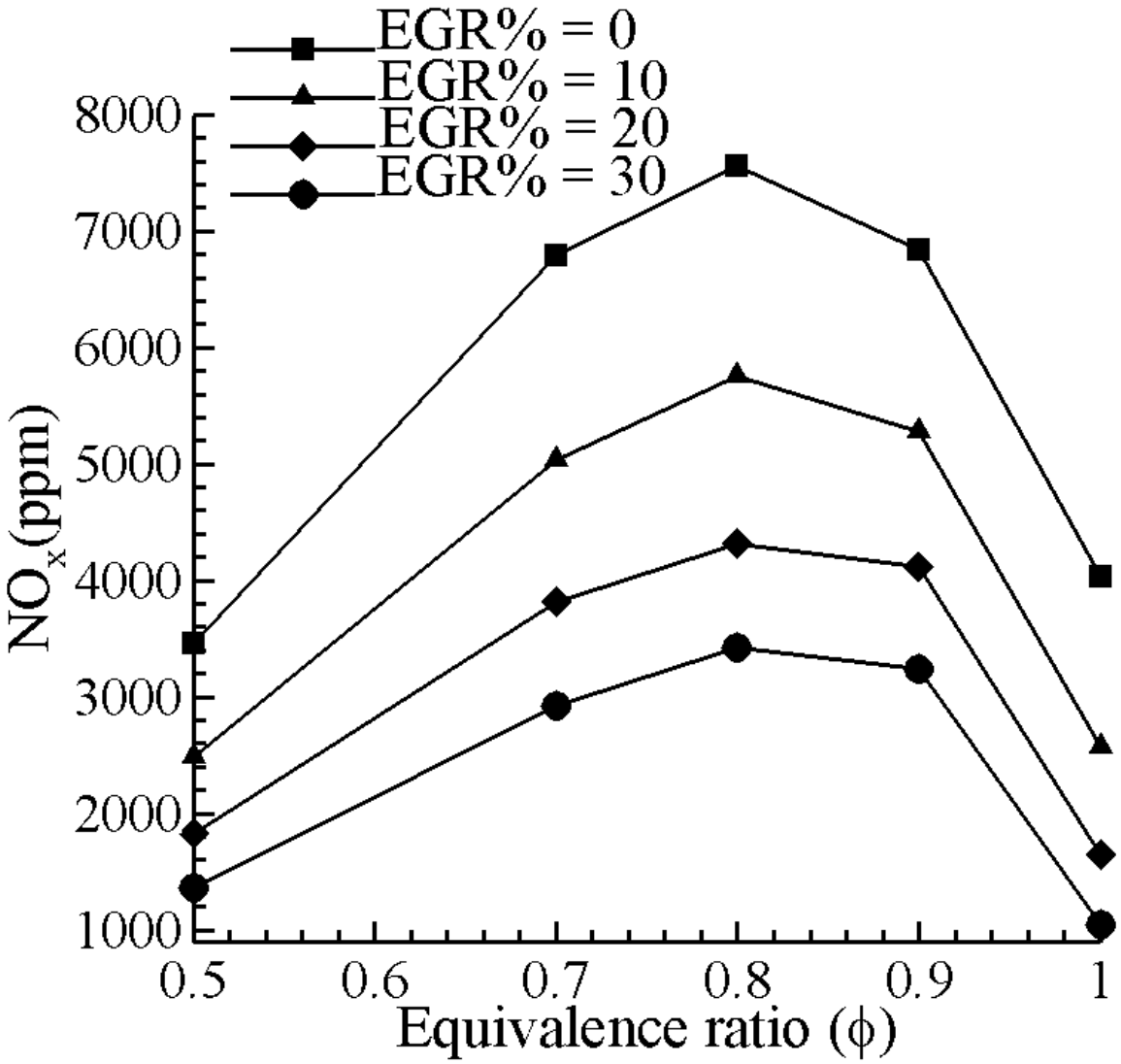

Figure 4: Effect of equivalence ratio (ϕ) and EGR fraction on NO_x formation.

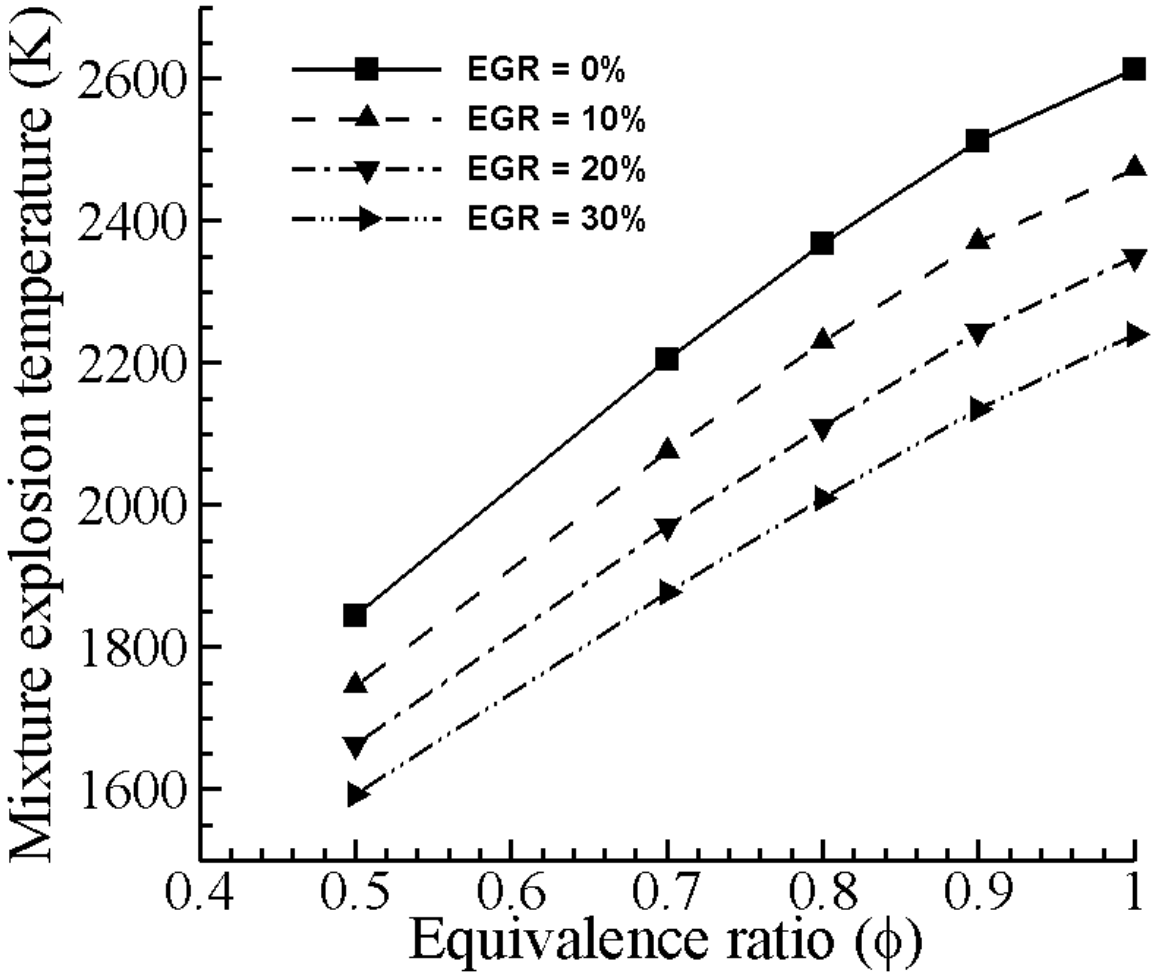

Figure 5: Effect of equivalence ratio on mixture equilibrium temperature for a range of EGR fractions.

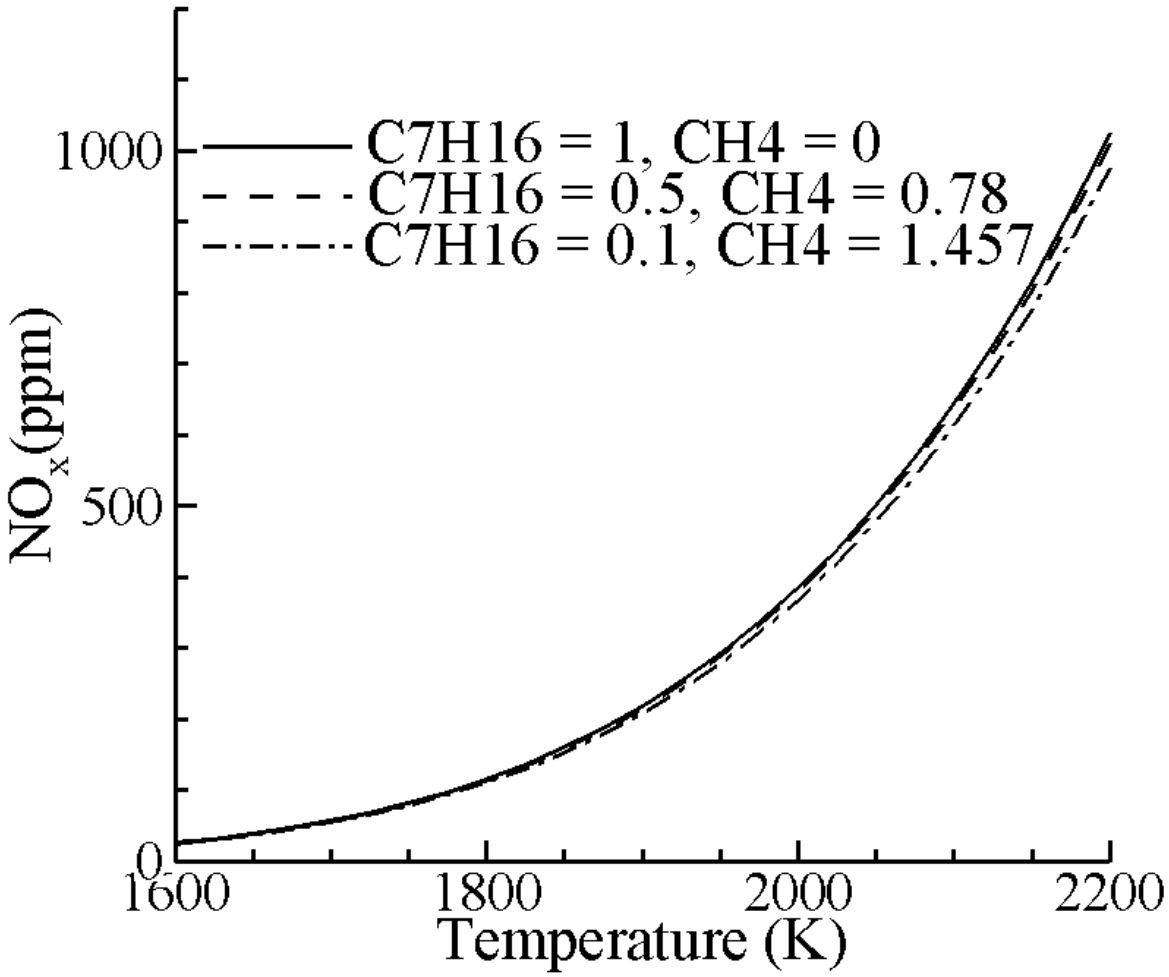

Figure 6: Variation of NO_x (ppm) with temperature for a natural-gas/diesel dual-fuel engine.

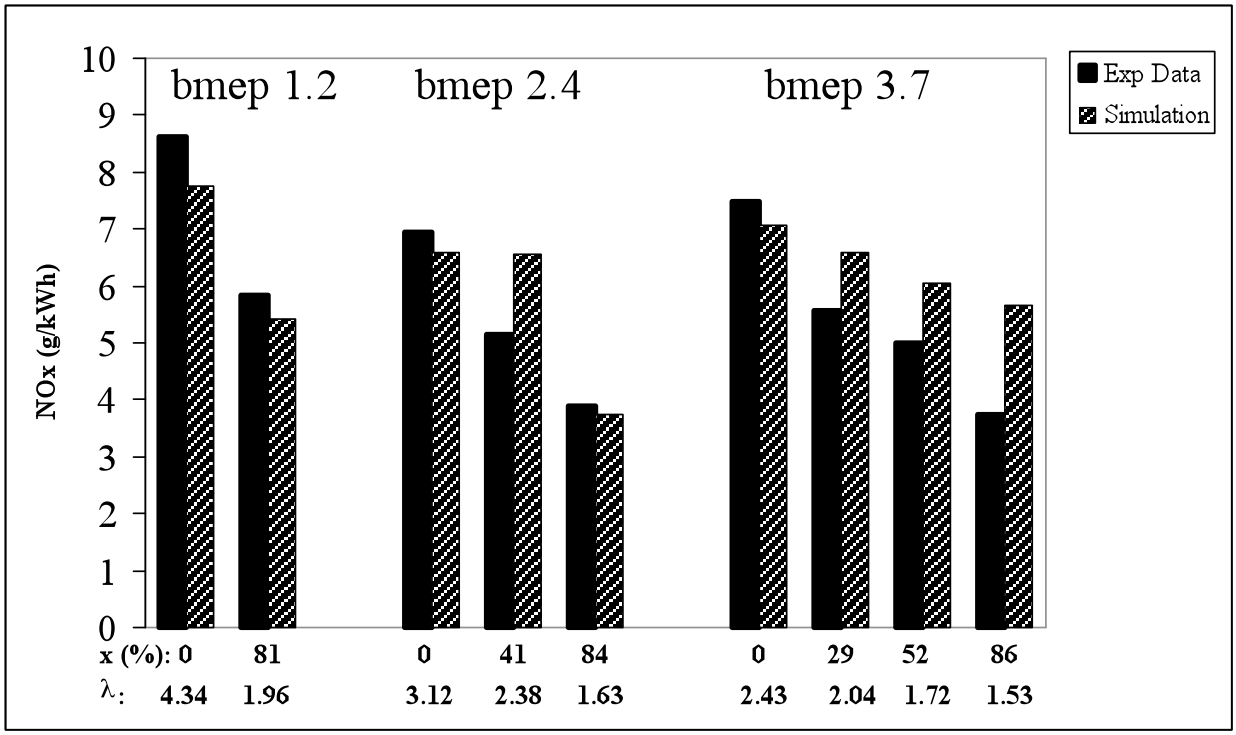

Figure 7: Comparison of predicted engine-out NO_x with experimental data [17].

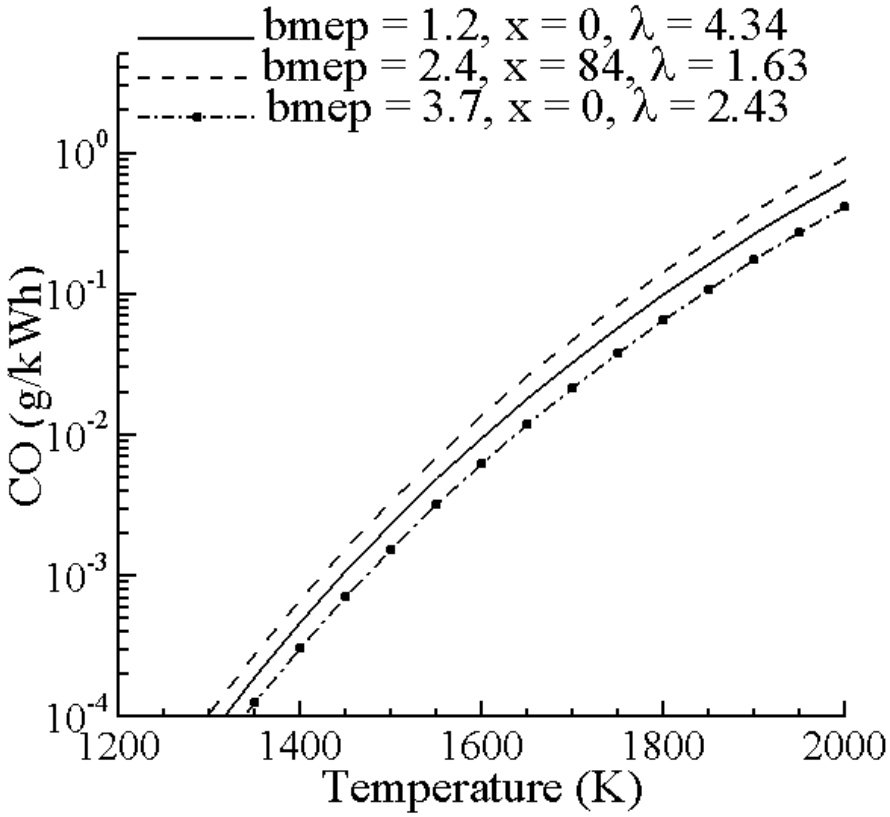

Figure 8: CO concentration for three values of load and mixture composition (x and λ).

List of Tables

List of figures: